Structure and phase diagram of strongly-coupled bipolar charged-particle bilayers

P. Hartmann[1], Z. Donkó[1] and G. J. Kalman[2]

[1] *Research Institute for Solid State Physics and Optics of the Hungarian Academy of Sciences - P.O. Box 49, H-1525 Budapest, Hungary*
[2] *Department of Physics, Boston College - Chestnut Hill, MA 02467, USA*

Abstract. – We report Monte Carlo simulations of a classical, strongly-coupled charged-particle bilayer with opposite charges in the two layers. At layer separations comparable to the Wigner-Seitz radius the two layers support each other to establish a quasi-long-range order; at low layer separations stable dipoles (classical equivalents of bound excitons) are formed and the long-range order is extinguished as the Coulomb interaction changes to a dipole-dipole interaction. We identify dipole-liquid, dipole-solid, Coulomb-liquid and Coulomb-solid phases, which are exhibited in an intuitive phase diagram of the system in the Γ (coupling)-d (layer separation) plane.

Introduction. – Bilayer systems of charged particles formed in semiconductor nanostructures have attracted a great deal of attention over the past decade [1]. In such systems charge carriers are confined within two quasi-two-dimensional layers. Sophisticated microelectronics techniques allow fabrication of both unipolar (electron-electron) and bipolar (electron-hole) bilayers characterized by different layer separation (d) and surface density (n) values. For certain domains of these parameters (and the system temperature) the classical description of the systems becomes quite adequate: *e.g.* in the strong-coupling domain —where the interaction energy of particles dominates over the kinetic energy [2]— the localization of the charges substantially reduces in-layer exchange effects.

In the case of unipolar systems (which are also relevant to particle traps [3]) the extra degree of freedom compared to the case of a single-layered system, gives rise to a rich variety of structural phases [4,5]. In bipolar systems it is expected that in an appropriate parameter domain the electrons and the holes bind to each other in a dipole-like excitonic formation [6–8]. It is also expected that at low enough temperatures the system undergoes a transition into a Wigner crystal-like solid phase [9]. The conflicting tendencies to undergo various transitions clearly affect each other: most importantly, the formation of bound dipoles reduces the long-range character of the (Coulombic) interparticle forces. The details of these processes are presently unclear. The aim of the present paper is thus to investigate the structural properties

of electron-hole bilayer systems over a wide range of system parameters within the limits of applicability of the classical approach. As we will show, the study reveals a rich variety of "phases" and an intricate "phase diagram" in the parameter space. It is, however, emphasized and should be kept in mind that the phase diagram is not derived on rigorous thermodynamic grounds and that the present simulations do not provide a detailed description of the character of the predicted phase transitions themselves. For each of these (possible) transitions extensive theoretical studies and additional computations are required that remain for future work.

Modeling approach. – The principal physical characteristics of the system of the two oppositely charged species physically separated from each other allows one to represent most of their physical properties through a classical modeling [9,10]. In a classical model the finite temperature of the system accounts for the kinetic energy of the particles and the system can be characterized by two dimensionless parameters: i) the plasma coupling parameter $\Gamma = e^2/(4\pi\epsilon_0 akT)$, where e is the charge of the particles, $a = (n\pi)^{-1/2}$ is the Wigner-Seitz (WS) radius and n is the surface density, and ii) the distance of layers d.

Our simulation method is based on the Metropolis Monte Carlo (MC) algorithm. The energy of the system is calculated by summation of the interaction energy over each pair of particles taking into account periodic images of the particles. The particle configuration with the lowest energy is searched for by random trial movements (in direction and displacement) of randomly chosen particles. At layer separations where the particles are strongly bound in dipole pairs, trial moves of particle pairs are also used. The quadrangular simulation cell contains $N = 400$ particles in each layer; the V(volume) $\to \infty$ condition is simulated by using periodic boundary conditions. The MC simulation code (modified for the unipolar case) has been cross-checked with a molecular-dynamics code [5]. It has also been verified that the present code is insensitive to the initial setting of the particle positions. The calculations cover
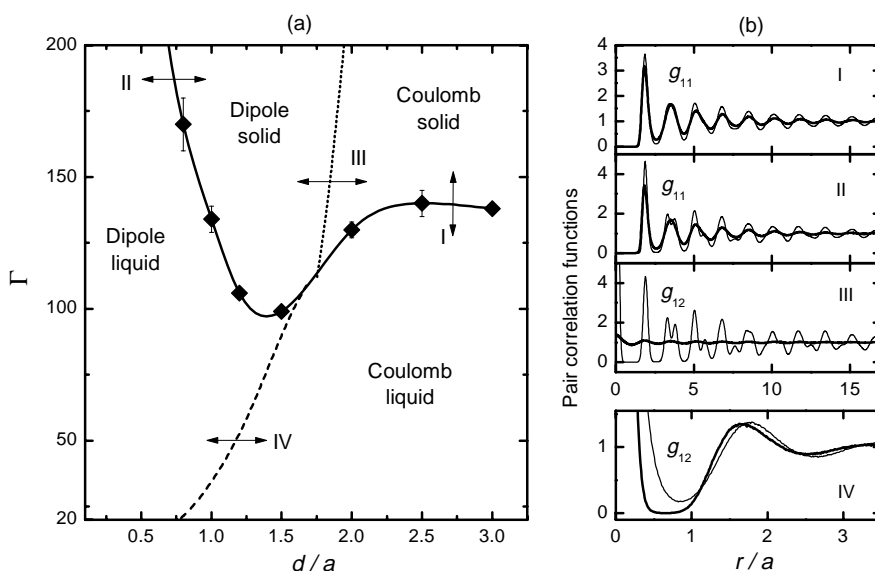
Fig. 1 – (a) Phase diagram of the bipolar bilayer system in the Γ-d/a plane. (b) Pairs of PCFs next to the two sides of the phase boundaries, indicating the characteristic changes that take place across the respective boundaries (marked with arrows in (a)) I: CL (heavy line)/CS (thin line), II: DL (h)/DS (t), III: CS (h)/DS (t), IV: DL (h)/CL (t).
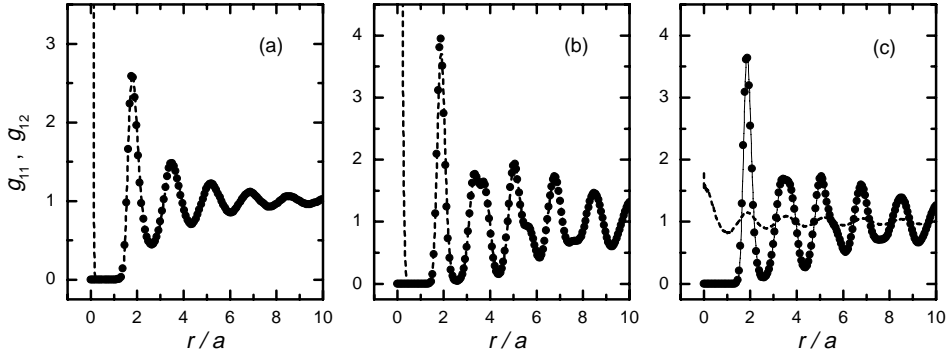
Fig. 2 – In-layer (g_{11}, symbols) and interlayer (g_{12}, dashed lines) PCFs as functions of r/a at $\Gamma = 150$. (a): $d/a = 0.6$ (DL); (b): $d/a = 1.2$ (DS); (c): $d/a = 2.0$ (CS).

the $20 \leq \Gamma \leq 200$ range of coupling values and layer separations $0.1 \leq d/a \leq 3.0$. We identify the phases by analyzing the in-layer $g_{11}(r)$ and interlayer $g_{12}(r)$ pair correlation functions (PCFs) and by calculating the diffusion coefficient as a function of the system parameters.

Results and discussion. –   As stated, our results reveal a rich variety of phases for the system. The ensuing phase diagram (fig. 1(a)) is governed by the competition between the strong in-layer Coulomb interaction favoring a long-range order and the interlayer attraction supporting the formation of stable dipole-like structures; these latter when formed tend to replace the Coulomb interaction by a weaker in-layer dipole-dipole potential. The various domains in the phase diagram can be tentatively recognized as representing Coulomb-liquid (CL), Coulomb-solid (CS), dipole-liquid (DL), and dipole-solid (DS) phases as shown in fig. 1(a).

Through scanning the Γ-d/a parameter space, several distinct features in the structures of the in-layer $g_{11}(r)$ and the interlayer $g_{12}(r)$ PCFs emerge, which can be recognized as unique signatures of the various phases in the parameter space. Figure 1(b) shows scans of $g_{11}(r)$ and $g_{12}(r)$ across tentative interphase boundaries. Typical $g_{11}(r)$ and $g_{12}(r)$ PCFs in the DL, DS, and CS domains are portrayed fig. 2.

The most conspicuous feature of the interlayer $g_{12}(r)$ PCF is that it develops a strong peak for low r/a values around $r = 0$, prevailing in the dipole domains, as can be observed in figs. 2(a) and (b). This behavior indicates the formation of (either permanent or temporary) dipole-like particle pairs. The height of this 0th peak of g_{12} increases with decreasing d/a as the attraction between the dipole-forming particles increases. Remarkably, the height $g_{12}(r = 0)$ for small d is approximately proportional to d^{-3} as shown in fig. 3(a) and not to $\exp[\Gamma/d]$, as would be expected on thermodynamic grounds. This can be understood by analyzing the normalization integral for $g_{12}(r)$. For the case of a bound dipole state the overwhelming contribution to the normalization integral C comes from the vicinity of the 0th peak and can be written as $C = I + V$, where

$$I = \pi \int_0^{r_0} r \exp\left[\frac{\beta e^2}{4\pi\varepsilon_0 \sqrt{r^2 + d^2}}\right] \mathrm{d}r = \pi d^2 \int_0^{x_0} x \exp\left[\frac{\Gamma}{\sqrt{1 + x^2}}\right] \mathrm{d}x, \qquad (1)$$

where r_0 is of the order of a, a distance where $g_{12}(r)$ drops to its normal value of O(1) (cf. fig. 2). V is the (2D) normalization volume, resulting from the integral from r_0 to ∞. The value of I can be easily obtained from the asymptotic expansion of the integral for $\Gamma\frac{a}{d} \to \infty$:

$$I \to 2\pi\frac{d^3}{\Gamma a} \exp\left[\Gamma\frac{a}{d}\right]. \qquad (2)$$
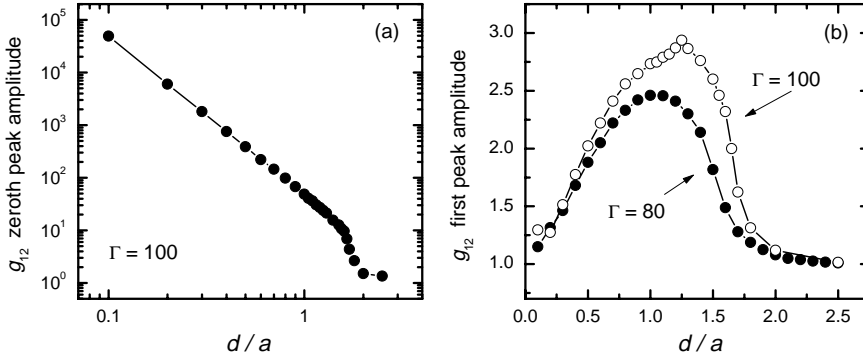
Fig. 3 – The amplitude of (a) the 0th (dipole), and (b) first peak of g_{12} as a function of d/a. $\Gamma = 100$ in (a) and $\Gamma = 80$ and 100 in (b).

In contrast to the case of a normal thermodynamic limit, where $I \ll V$, here, for any reasonable choice of parameters, V is negligible and $g_{12}(r = 0) \propto V/I \propto \Gamma/d^3$.

In the DL and DS domains the $g_{11}(r)$ and $g_{12}(r)$ functions are identical (in contrast to their behavior in CL and CS), except for the 0th peak discussed above, as shown for DL and DS in fig. (2). This is an indication that in these domains the dipole-forming particles lock into a permanent formation. This interpretation is corroborated by the snapshots of particle positions, shown in figs. 4(a) and (b). It is clear that both at layer separation $d/a = 1.2$ (Fig. 4(a)), where the dipoles form an ordered hexagonal structure, and at very low separation $d/a = 0.2$, where the positions of the dipoles are largely randomized, and their positions are not fixed (fig. 4(b)), oppositely charged particles are bound to each other. In the same DL and DS domains the $g_{12}(r)$ interlayer PCF exhibits in the range of r between the fall-off of its 0th peak (dipole peak) and the first peak (first neighbor's peak) a correlation void where $g_{12}(r) = 0$ (see fig. 1(b)/III and IV). This void evidences that there is no exchange of particles between neighboring dipoles. Thus we have clear indications that it is justified to characterize the D-phases as being constituted of permanently bound dipoles. To illustrate the onset of
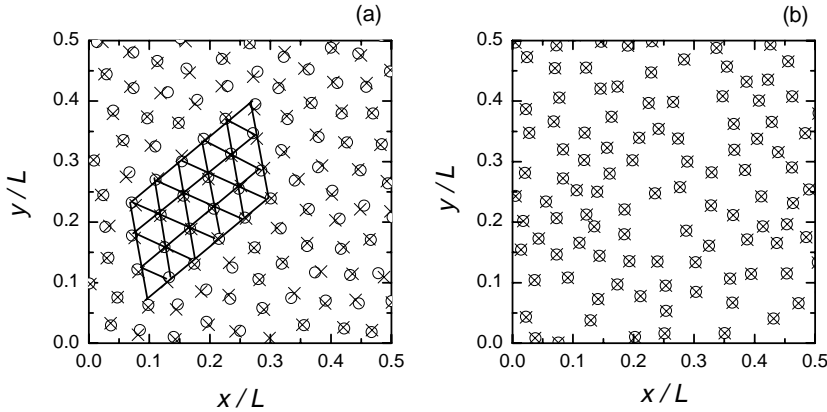
Fig. 4 – Snapshots of particle positions at $\Gamma = 100$, (a) $d/a = 1.2$ and (b) $d/a = 0.2$. The positions of particles in the two layers are indicated by circles and crosses, respectively. Note that in (b) the particle positions visually completely coincide.
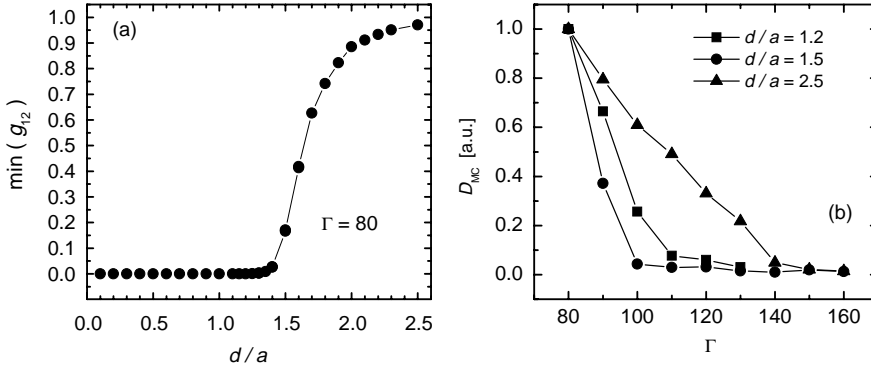
Fig. 5 – (a) First minimum of $g_{12}(r)$ as a function of layer separation for $\Gamma = 80$. (b) Normalized D_{MC} as a function of Γ for selected values of d/a. The normalization factor is chosen that $D_{\mathrm{MC}}(\Gamma = 80) = 1.0$.

the transition from dipole liquid to Coulomb liquid (DL → CL) we plot in fig. 5(a) the value of the first minimum of $g_{12}(r)$ across the DL-CL boundary as a function of layer separation d/a. One can observe the dramatic rise of this value from zero as d/a is slightly increased.

At high layer separations, in domain CL, $d/a \geq 2.0$, there is no appreciable interlayer correlation, and the two layers behave independently, similarly to a 2D one-component plasma (OCP). When the separation of the two layers is decreased, a strong enhancement of the first peak of $g_{12}(r)$ can be observed. This is shown in the $\Gamma = 80$ and $\Gamma = 100$ scans in fig. 3(b). At intermediate separations ($d/a \cong 1$) the two layers support each other to establish a quasi-long-range order. This behavior is similar to that of the unipolar bilayer where an enhanced correlation [5] and higher melting temperature [11] has also been found for intermediate (although somewhat lower) layer separations. When the two layers further approach each other the system transform into dipole liquid (DL) phase and the trend for the formation of an enhanced correlation peak is reversed: for $d/a \leq 1.2$ the in-layer correlation rapidly decreases. This behavior is an indication of the change of the long-range Coulomb force into a short-range dipole-dipole interaction.

A salient feature of the change both from the DL into the DS and from the CL into the CS domains is the emergence of a quasi-long-range order. This is demonstrated in fig. 1(b)/I and II, where PCFs calculated near these liquid-solid phase boundaries are shown. The correlation function changes drastically, showing the onset of the long-range order when the interlayer separation is slightly increased at constant Γ.

While the long-range order prevails both in the DS and CS phases, as shown through the portrayal of the similar $g_{11}(r)$ PCFs in figs. 2(b), (c), there is a strong difference between the two interlayer $g_{12}(r)$ PCFs: an abrupt reduction of the interlayer PCF as the system changes from the DS phase to a CS phase ensues (see fig. 1(b)/III). Analysis of the coordination numbers associated with the PCFs shows that the lattice structure in the DS and the CS solid phases and the underlying structure in the CL and DL liquid phases are always hexagonal and do not change with changing layer separation (in contrast to unipolar bilayers [4,5]).

The interpretation of the transition from the DL into the DS and from the CL into the CS phases, respectively, as a liquid-solid phase transition is further supported by the calculation within the MC simulation of the quantity [12]: $D_{\mathrm{MC}} = \frac{1}{k} \langle \left[\boldsymbol{r}(k) - \boldsymbol{r}(0) \right]^2 \rangle$, where k is the number of MC steps. D_{MC} is analogous to the diffusion coefficient in "real-time" (*e.g.* MD)

simulations. Although time does not appear in the MC simulation, D_{MC} can distinguish between the diffusive/non-diffusive state of the system [13]. Figure 5(b) shows normalized D_{MC} as a function of Γ, for selected values of d/a. At all values of d/a there exists a marked drop of "diffusion" at a certain value $\Gamma = \Gamma_{\mathrm{m}}$. At high separation, Γ_{m} approaches the value 137, characterizing the melting of the 2D one-component plasma (OCP).

An additional indicator of the phase change can be provided by observing the bond-angular correlations, which has been shown to develop a sudden drop across the solid-liquid melting line (see, *e.g.*, [11]). We have verified that the bond-angular order parameter indeed exhibits this expected behavior (both in the Coulomb and dipole systems), at Γ_{m} values (depending on d/a), which are in good agreement with the data obtained from the diffusion analysis. We note that the transition from the CL to the DL phase, if it is indeed abrupt, should be a Metal/Insulator transition, with a corresponding change in the characteristics of the dielectric response function.

It should be clear that on the basis of the analysis presented here we cannot claim that the phase domains and phase boundaries in the diagram represent genuine thermodynamic phases and phase transitions: such a determination would require more detailed investigations, for example the study of the free energy functional, which is beyond the capabilities of our current MC simulation technique. With this proviso, we now summarize the features of the phase behavior of the system. At high d/a values the system behaves as a combination of two independent 2D OCPs and the boundary between the CL and CS phases is at $\Gamma_{\mathrm{m}} \approx 137$ (cf. fig. 1(b)/I). With decreasing d/a, Γ_{m} decreases and reaches its minimum value $\Gamma_{\mathrm{m}} \approx 100$ at $d/a = 1.4$. The fact that the lowest Γ_{m} is found at intermediate layer separations is similar to the behavior of the classical electronic bilayers [11]. Below $d/a = 1.4$, Γ_{m} increases again and reaches very high values as the layer separation decreases. This effect is caused by the decrease of the coupling between neighboring particle pairs, as the Coulomb potential changes to a dipole-dipole potential at low layer separations. To describe the interaction between the dipoles the Coulomb coupling parameter $\Gamma \propto e^2/akT$ is to be replaced by a coupling parameter for dipoles, $\Gamma_{\mathrm{D}} \propto e^2 d^2/a^3 kT = \Gamma(d/a)^2$. If we assume that the freezing occurs at some characteristic value of $\Gamma_{\mathrm{D}} \approx \Gamma_{\mathrm{D}0}$, then Γ_{m} should behave as $\Gamma_{\mathrm{D}0}(d/a)^{-2}$ as $(d/a) \to 0$. In fact, for $d/a < 1$ the phase boundary is well approximated by the above expression, with $\Gamma_{\mathrm{D}0} = 75$. This boundary now separates the DL and DS phases (cf. fig. 1(b)/II). Thus at low d/a values it is always the DL phase that prevails. For high Γ values, increasing d/a across the DS region leads to the DS/CS boundary (cf. fig. 1(b)/III). At lower Γ values this boundary separates the DL from the CL phases (cf. fig. 1(b)/IV). The explanation of the way these boundaries form is as follows. When the energy δE needed to displace the two hexagonal lattices with respect to each other becomes smaller than the thermal energy kT (related to Γ), the two lattices are no longer locked into each other. With increasing layer separation δE rapidly decreases, and thus it has to be balanced by a matching increase of Γ. A similar explanation applies to the boundary separating the DL and CL phases.

The precise behavior of the system in the region within which the solid/liquid and dipole/Coulomb boundaries cross has not been resolved to the degree of precision that would warrant a statement as to the nature of that region.

Our phase diagram may be compared with the recently calculated quantum Monte Carlo (QMC) phase diagram of an electron-hole bilayer at zero temperature by De Palo, Rapisarda and Senatore (DRS) [7]. DRS distinguish three phases, labeled as the excitonic phase (EP), 2 Coulomb plasma (2CP) and Wigner crystal (WC) phases, in one-to-one correspondence with our DL/DS, CL and CS phases. In DRS there is no attempt to resolve liquid *vs.* solid excitonic phases. Their triple point (found at $d/a = 1.3$) is in the vicinity of the region where the phase boundaries cross in the present work; the ratio of the corresponding r_s (quantum

coupling coefficient) value (≈ 20) and Γ value (≈ 95) is similar to the ratio of the 2D freezing r_s/Γ ratio (37/137) and reflects the fact that the electron liquid freezes with a higher relative kinetic energy than its classical counterpart. Filinov *et al.* [8] have also generated a QMC phase diagram for a mesoscopic electron-hole bilayer and have identified the excitonic crystal phase. They have concluded that their phase diagram compares favorably with ours.

Summary. – In summary, we have analyzed through MC simulation the phases of a classical bipolar bilayer. We have shown that at low layer separation the particles combine into stable bound dipole pairs (classical equivalents of bound excitons), destroying the quasi-long-range order and forming a dipole liquid. Increase of the layer separation or increase of the coupling parameter converts the dipole liquid into a dipole crystal. We have also exhibited the adjacent parameter domains where the two charge species still behave as quasi-independent components of two strongly coupled Coulomb systems.

$$* * *$$

REFERENCES

[1] FUKUZAWA T., MENDEZ E. E. and HONG J. M., *Phys. Rev. Lett.*, **64** (1990) 3066; SIVAN U., SOLOMON P. M. and SHTRIKMAN H., *Phys. Rev. Lett.*, **68** (1992) 1196; TSO H. C. and VASILOPOULOS P., *Phys. Rev. Lett.*, **70** (1993) 2146; PARLANGELI A., CHRISTIANEN P. C. M., GEIM A. K., MANN J. C., EAVES L., MAIN P. C. and HENINI M., *Physica B*, **256-258** (1998) 531; CONTI S., VIGNALE G. and MACDONALD A. H., *Phys. Rev. B*, **57** (1998) R6846.

[2] KALMAN G. J., ROMMEL J. M. and BLAGOEV K. (Editors), *Strongly Coupled Coulomb Systems* (Plenum Press, New York) 1998.

[3] MITCHELL T. B., BOLLINGER J. J., DUBIN D. H. E., HUANG X. P., ITANO W. M. and BAUGHMAN R., *Science*, **282** (1988) 1290.

[4] VALTCHINOV V., KALMAN G. J. and BLAGOEV K. B., *Phys. Rev. E*, **56** (1997) 4351.

[5] DONKÓ Z. and KALMAN G. J., *Phys. Rev. E*, **63** (2001) 061504.

[6] LITTLEWOOD P. B. and ZHU X., *Phys. Scr. T*, **68** (1996) 56.

[7] DE PALO S., RAPISARDA F. and SENATORE G., *Phys. Rev. Lett.*, **88** (2002) 206401; SENATORE G. and DE PALO S., *Contrib. Plasma Phys.*, **43** (2003) 363.

[8] FILINOV A. V., LUDWIG P., GOLUBNYCHNYI V., BONITZ M. and LOZOVIK YU. E., *Phys. Status Solidi (c)*, **0** (2003) 1518; FILINOV A. V., BONITZ M. and LOZOVIK YU. E., *J. Phys. A*, **36** (2003) 5899.

[9] KULAKOVSKII D. V., LOZOVIK YU. E. and CHAPLIK A. V., *J. Exp. Theor. Phys.*, **99** (2004) 850.

[10] OLIVARES-ROBLES M. A. and ULLOA S. E., *Phys. Status Solidi (b)*, **233** (2002) 280.

[11] SCHEWEIGERT I. V., SCHEWEIGERT V. A. and PEETERS F. M., *Phys. Rev. Lett.*, **82** (1999) 5293.

[12] TOTSUJI H., *Phys. Plasmas*, **8** (2001) 1856.

[13] VAULINA O. S. and VLADIMIROV S. V., *Phys. Plasmas*, **9** (2002) 835. VAULINA O., KHRAPAK S. and MORFILL G., *Phys. Rev. E*, **66** (2002) 016404. LIU B., LIU Y.-H., CHEN Y.-P., YANG S-Z. and WANG L., *Chin. Phys.*, **12** (2003) 765.